A Mathematical Model for Driver and Pedestrian Interaction in Shared Space Environments

Research · May 2015

DOI: 10.13140/RG.2.1.4670.6086

1 author:

Bani Anvari
University College London
29 PUBLICATIONS **192** CITATIONS

SEE PROFILE

A Mathematical Model for Driver and Pedestrian Interaction in Shared Space Environments

Ms Bani Anvari

PhD Candidate

Imperial College London
Department of Civil & Environmental Engineering
Centre for Transport Studies
Imperial College Road
London SW7 2BU
United Kingdom

Abstract

The shared space concept develops a slow and safe environment with promoting a sense of vigilance and responsibility. This is achieved by reducing demarcation and any physical distinctions between the streets and pedestrian areas. However, there is a need to identify the conditions under which shared space is a feasible alternative to traditional controlled traffic designs. Predicting and visualising the responses of pedestrians to the behaviour of drivers, neighbouring pedestrians or obstacles in a shared environment is important from the standpoint of traffic management. Thus, a microscopic model based on the Social Force Model (SFM) is developed for shared space users. Since human beings aim is to follow the shortest path in order to reach their destination, this feature is added using the Distance Potential Field. This mathematical approach is meant to be the fundamental framework for a future simulation of shared space users. In order to calibrate this new modified SFM, parameters are initialised based on the observation made from New Road in Brighton. The paper presents a calibration approach and describes how to evaluate the results.

Keywords: Shared Space, Social Force Model, Pedestrian, Vehicle, Simulation, Calibration

1 Introduction

Public space design has moved towards space sharing similar to ”Woonerf” schemes in western countries over the last century (Shearer, 2010). Shared space can be defined as any type of road design that removes some or all separations between road users and reduces traffic control infrastructure (Reid et al., 2009). The objective is to raise pedestrian priority and establish a shared space dynamic within the street to modify drivers' behaviour (Hamilton-Baillie, 2008). These redesigning streetscapes contribute to an increase in the community texture and an improvement in social interactions (Gilman and Gilman, 2007). In order to achieve these aims, street designers and traffic engineers need to understand the dynamics of traffic flow with the lack of traffic control. A mathematical description of this process opens the possibility to analyse the dynamics of pedestrian and driver streams in shared areas to be designed. This can support infrastructure designers to optimise their design, making it more efficient, more comfortable, safer and adapted to different activities. Therefore, this paper investigates a space continuous model to describe the shared space dynamics quantitatively over time.
In Section 2, the mathematical model of vehicular, pedestrian and pedestrian-vehicular dynamics is reviewed. Section 3 provides a background on the Social Force Model (SFM). The

new mathematical model is presented in Section 4. The need for observation, the calibration methodology and the collected microscopic data from a shared street in Brighton (United Kingdom) is explained in Section 5.

2 Background

A theoretical model predicting pedestrian and driver flow patterns, travel times, speeds etc. is important in order to identify the conditions under which sharing space is a feasible alternative to traditionally controlled traffic systems. Researchers have developed mathematical theories modelling vehicular traffic, pedestrian motion and mixed traffic in three scale levels: microscopic, mesoscopic and macroscopic. The goal of this study is to introduce a microscopic mathematical model that can reproduce the main observable behaviours. Therefore, a review of the models for vehicular traffic, pedestrian dynamics and pedestrian-vehicle mixed traffic is given below.

Vehicular traffic models attempt to define the behaviour of a traffic stream by describing the behaviour of individual drivers in different situations. Drivers have to control the vehicle position along the direction of motion and the vehicle's position across the width of the road or lane. Both of these activities are mutually dependent. A typical theory is the car-following model (McDonald, 1999; Newell, 2002; Zhang and Kim, 2005). Bando et al. (1995) presented the optimal velocity model (OVM) which assign an optimal velocity function dependant on the headway of each vehicle to explain different characteristics of traffic flow. Helbing and Tilch (1998) explained that OVM can result in unrealistic accelerations and proposed the generalized force model (GFM) to solve the problem. Jiang et al. (2001) pointed out that the GFM show poor delay time of motions and kinematic wave velocities at jam density. They proposed a full velocity difference model (FVDM) on the basis of GFM by considering the positive velocity differences. Further, Intelligent Transport Systems (ITS) have been proposed involving the use of vehicle-to-vehicle information to improve the stability of traffic flow and stop traffic jams. For instance, some studies have been done by considering multiple headways of preceding or following cars (Xie et al., 2009; Ge et al., 2006, 2005) as well as considering the effect of multiple velocity differences of preceding cars based on the full velocity model (Lia and Liu, 2006).

The mathematical structure for modelling pedestrian dynamics is similar to vehicular traffic. The difference is that pedestrians move in more than one space dimension. Rule based models display pedestrian movement in space based on observed behavioural rules. Thus, these models divide the map into discrete spaces, as in the case of Cellular Automata Models (CA). The CA models have been used in the simulation of pedestrian flows by Yu and Song (2007); Franca et al. (2009), and Ishii and Morishita (2010).
Force based models define the pedestrians' movement as the resolution of the social forces exerted by other individuals and obstacles. The sum of all the forces persuades the movement and its direction which is described by the SFM (Helbing, 1991) and the Centrifugal Force Model (Yu et al., 2005; Chraibi and Seyfried, 2010). Force-based models can describe trajectories and velocities since their parameters are associated with meaningful quantities that can be measured. In addition, they can be modified to allow different behaviours or actions for new scenarios (Seyfried et al., 2005; Moussad et al., 2009).

Concerning mixed pedestrian-vehicle flows over a network, limited number of studies have been reported in the literature. Among those, Helbing et al. (2005) formulated and analysed the interaction of pedestrians with vehicles in the macroscopic level. Jiang and Wu (2006) explored a simple lattice gas model to study the vehicle and pedestrian flows in a narrow

channel. Ishaque and Noland (2007) studied the pedestrian traffic with VISSIM, where vehicle and pedestrian modes are operated independently and controlled by the traffic signals at potential conflicting areas.

Therefore, this study will attempt to address pedestrian-vehicular mixed traffic with the use of the SFM. The proposed mathematical model has integrated the strengths of the SFM and experimental results of New Road in Brighton is used to support the behavioural assumptions for the shared space simulation.

3 Social Force Model

The SFM was implemented by Helbing (1991), Helbing and Molnar (1995), and Helbing et al. (2000) by using the concept of the social force or social field (Lewin, 1951). People are presented as single particles moving on a plane, and interacting with boundaries and each other if coming in close contact. This behaviour is determined by Newtons second law of dynamics as a guiding principle. The movement of each pedestrian by assuming the unit mass is described by:

$$\frac{d\vec{v}_\alpha(t)}{dt} = \vec{f}_\alpha^0 + \sum_{\beta(\beta\neq\alpha)} \vec{f}_{\alpha\beta} + \sum_b \vec{f}_{\alpha b} + \sum_i \vec{f}_{\alpha i} + \sum_{\beta(\beta\neq\alpha)} \vec{f}_{\alpha\beta}^{\,\mathrm{att}} + \vec{\xi} \tag{1}$$

In the Social Force Model, motivations of movement are modelled as forces. For instance, the motivation of pedestrian α to avoid an obstacle b such as a wall or another pedestrian β are modelled as social repulsive forces $\vec{f}_{\alpha b}$ and $\vec{f}_{\alpha\beta}$, the motivation to orient his direction toward a certain object β is modelled as a social attractive force $\vec{f}_{\alpha\beta}^{\,\mathrm{att}}$. Finally, the motivation to adapt his velocity to another velocity he prefers to move at is modelled as a driving force $\vec{f}_\alpha^0$. Here, the social forces have magnitudes and directions similar to the physical forces. A more detailed description can be found in (Helbing, 1991; Helbing and Molnar, 1995; Helbing et al., 2000).

4 Microscopic Model for Shared Space Users

The new microscopic model presented in this section is based on Helbing's SFM. Since, a new element (the vehicle) needs to be added, the new arrangement integrating a vehicle γ is shown in Figure 1. The sum of the force terms exerted from a pedestrian α, a boundary b and

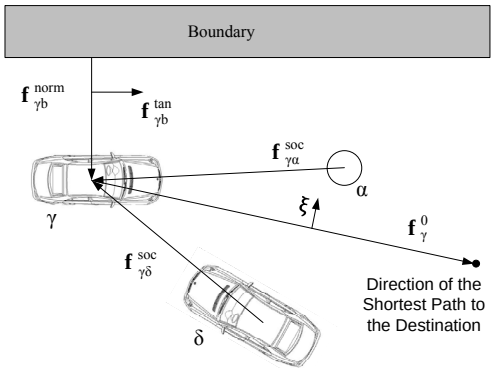

Figure 1: Force Term Exterted to a Car from a Pedestrian/Car/Boundary

another vehicle δ can be seen in the Equation 2 as well. Each summand will be explaind in

more detail in the following sections.

$$\frac{d\vec{v}_\gamma(t)}{dt} = \vec{f}_\gamma^0 + \sum_{\alpha(\alpha\neq\gamma)} \vec{f}_{\gamma\alpha}^{\text{soc}} + \sum_{\delta} \vec{f}_{\gamma\delta}^{\text{soc}} + \sum_{b(b\neq\gamma)} \vec{f}_{\gamma b} + \vec{\xi} \tag{2}$$

4.1 Driving Force

The driving force for a car is similar to the one applied for pedestrians as this force term is the motivation to move towards a certain destination. Therefore, the driver γ is assumed to move in a desired direction $\vec{e}_\gamma^0$ with a desired speed v_γ^0 that is adapted to the actual velocity $\vec{v}_\gamma$ within a certain relaxation time τ_γ.

$$\vec{f}_\gamma^0 = \frac{v_\gamma^0 \cdot \vec{e}_\gamma^0(t)}{\tau_\gamma} - \frac{\vec{v}_\gamma}{\tau_\gamma}, \text{ where } \vec{e}_\gamma^0(t) = \frac{\vec{d_\gamma} - \vec{x_\gamma}}{|\vec{d_\gamma} - \vec{x}_\gamma|} \tag{3}$$

The desired direction $\vec{e}_\gamma^0$ above is estimated from the momentary location of the car and the desired destination $\vec{d}_\gamma^0$.

4.2 Geometric Model for Cars and their Interaction Forces

The interaction between a car and nearby pedestrians is described by a socio-psychological force $\vec{f}_{\gamma U}$.

$$\vec{f}_{\gamma U}^{\text{soc}} = A_{\gamma U} e^{\frac{r_{\gamma U} - d_{\gamma U}}{B_{\gamma U}}} \vec{n}_{\gamma U} F_{\gamma U} \tag{4}$$

Here, $\vec{f}_{\gamma U}^{\text{soc}}$ represents the interaction of the car γ either with another car ($U = \delta$) or with a pedestrian ($X = \alpha$). In addition, $\vec{n}_{\gamma U}$ is the normalized vector pointing from another user (car or pedestrian) to car γ and parameters $A_{\gamma U}$ and $B_{\gamma U}$. Since the form factor and the radii will be different from the one for pedestrians, these factors have to be redefined. In normal situations, vehicles will not touch each other, which is equivalent to a collision, and therefore, they do not exert a physical force. Contrary to a circle with a radius r_α along the distance from another

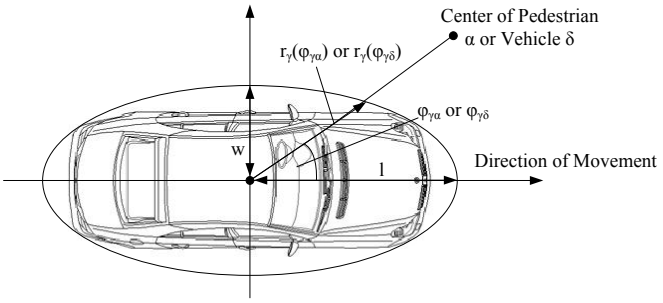

Figure 2: Vehicle Modelling using a Geometrical Approximation of an Ellipse

pedestrian, that is assumed for a pedestrian α in the Social Force Model, an ellipse with radius r_γ can be modelled for a car (Figure 2). The radius r_γ depends on the angle $\varphi_{\gamma U}$ between the desired direction of a car and the direction of the close-by pedestrian or car who is exerting a force. The radius of the elipse $r_\gamma(\varphi_{\gamma U})$ in polar coordinates is as follows:

$$r_\gamma(\varphi_{\gamma U}) = \frac{w}{\sqrt{1 - \epsilon^2 cos^2(\varphi_{\gamma U})}}, \text{where } \epsilon = \frac{\sqrt{l^2 - w^2}}{l} \tag{5}$$

In Equation 5, $2l$ and $2w$ are assumed to be the average length and width of a modelled car. Sum of the radii is therefore $r_{\gamma U} = r_\gamma + r_U$ and $d_{\gamma U}$ is the distance between the center of

car γ and another shared space user(car or pedestrian). The form factor $F_{\gamma U}$ is used to only consider forces pedestrians and cars within the angle of view exertec by of the driver behaviour. Considering that car movement is restricted to change of direction, and lateral movement is not possible for them, an effective field of view is introduced. The driver's view angle is compared to the effective field of view in Figure 3. However, there is a difference between a pedestrian

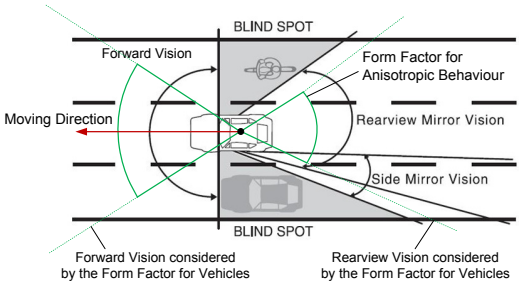

Figure 3: Effective Field of View Compared to Driver's Vision

and another car following a car since the leading car driver will only react to cars behind. This is expressed by:

$$F_{\gamma U} = \left(\lambda_\gamma + (1-\lambda_\gamma)\frac{1+cos(\varphi_{\gamma U})}{2}\right)\cdot q, \tag{6}$$

where q is the 'effective factor' that will distinguish between a car-pedestrian or a car-car interaction. Considering a car-car interaction, the following can be summarised for q:

$$\begin{aligned} q &= 1, \quad \text{if } -\vartheta^{\mathrm{o}} \leq \varphi_{\gamma\alpha} \leq \vartheta^{\mathrm{o}} \text{ and } (180^{\mathrm{o}} - \vartheta^{\mathrm{o}}) \leq \varphi_{\gamma\alpha} \leq (180^{\mathrm{o}} + \vartheta^{\mathrm{o}}) \\ q &= 0, \quad \text{otherwise} \end{aligned} \tag{7}$$

Figure 4a visualises the form factor $F_{\gamma\delta}$. By varying λ_γ, the influence of exerted forces of the cars behind the leading car changes.
Regarding a car-pedestrian interaction, q will be as follows, which is illustrated in Figure 4b.

$$\begin{aligned} q &= 1, \quad \text{if } -\vartheta^{\mathrm{o}} \leq \varphi_{\gamma\alpha} \leq \vartheta^{\mathrm{o}} \\ q &= 0, \quad \text{otherwise} \end{aligned} \tag{8}$$

The interaction between cars and boundaries/obstacles is described below by considering that

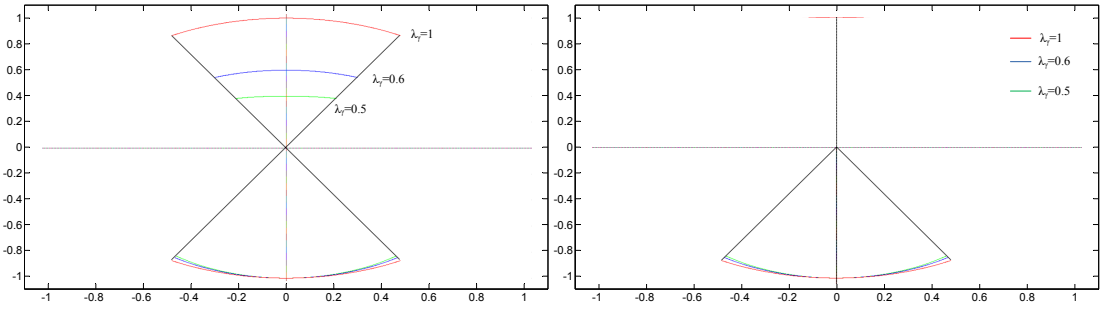

(a) Regarding Cars using $\vartheta = 30^{\mathrm{o}}$ (b) Regarding Pedestrians using $\vartheta = 30^{\mathrm{o}}$

Figure 4: Form Factor for Anisotropic Vehicle Behaviour

cars are not expected to have any physical contact with boundaries or obstacles. Therefore, an expression similar to Equation 4 is defined to avoid car accidents:

$$\vec{f}_{\gamma b} = A_{\gamma b} e^{\frac{r_\gamma - d_{\gamma b}}{B_{\gamma b}}} \vec{n}_{\gamma b} F_{\gamma b} \tag{9}$$

Here, $\vec{n}_{\gamma b}$ is the normal vector to the surface of a boundary or obstacle. Also, $d_{\gamma b}$ is the distance between a car centre γ and the closest vertex of boundary/obstacle polygon and it is calculated similar to the distance between a pedestrian and a boundary/obstacle. $F_{\gamma b}$ is also the form factor regarding car-boundary interactions similar to car-pedestrian interactions.

4.3 Relation between Steering Angle and Moving Velocity

As mentioned in Section 2, vehicles have restricted lateral movement. These limitations needs to be defined within the model. Regarding pedestrians, the angle of movement can be within $[0, 2\pi]$, whereas the maximum velocity should be limited to $v_\alpha(t) = 5.4\,\frac{\mathrm{km}}{\mathrm{h}}$. In respect of cars, not only the velocity is restricted to $20\,\frac{\mathrm{miles}}{\mathrm{h}}$ $(32\,\frac{\mathrm{km}}{\mathrm{h}})$, but also the angle of steering is limited. As shown in Figure 5a, the limitation function can be described as $v_{\gamma\mathrm{empirical}}(\psi_{car})$, where $\psi = arctan\left(\frac{v_{\gamma 2}}{v_{\gamma 1}}\right)$ is called the steering angle. This function will be determined considering empirical values. Figure 5b illustrates the same concept in polar coordinates and Equation 2 gives the resulting angle of movement and the velocity by computing $\vec{v}_\gamma(t)$. So, it is necessary

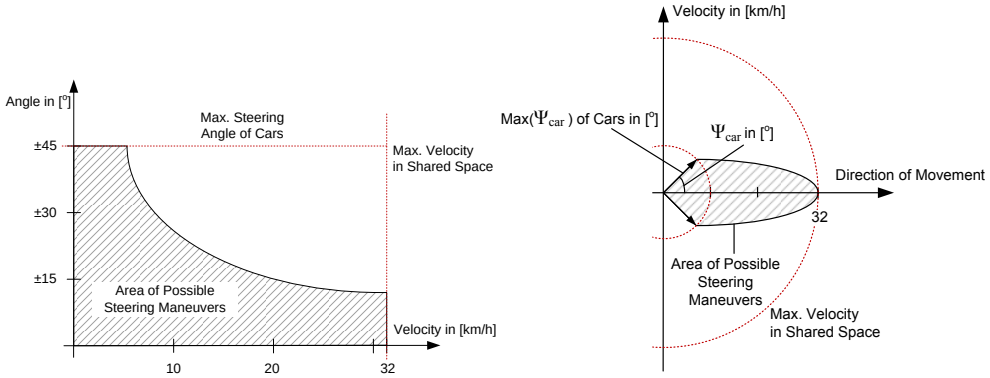

(a) Velocity versus Steering Angle (b) Steering Maneuvors in a Polar Coordinates

Figure 5: Vehicle Velocity versus Steering Angle

to constrain Equation 2. On the one hand the steering angle ψ should be within the interval $[0, \pm max(\psi_{\mathrm{car}})]$ and $v_\gamma(t)$ should not exceed a certain limit depending on ψ. Taking this into consideration, everything can be summarised having the following conditions:

$$\begin{aligned} \text{if} \quad & \psi_\gamma \geq max(\psi_{\mathrm{car}}) \wedge v_\gamma(t, \psi_\gamma) \leq v_\gamma(t, max(\psi_{\mathrm{car}})), \\ \text{then} \quad & \psi_\gamma = max(\psi_{\mathrm{car}}) \\ \text{if} \quad & \psi_\gamma \leq -max(\psi_{\mathrm{car}}) \wedge v_\gamma(t, \psi_\gamma) \leq v_\gamma(t, -max(\psi_{\mathrm{car}})), \\ \text{then} \quad & \psi_\gamma = -max(\psi_{\mathrm{car}}) \end{aligned} \tag{10}$$

$$\begin{aligned} \text{if} \quad & \psi_\gamma \geq max(\psi_{\mathrm{car}}) \wedge v_\gamma(t, \psi_\gamma) \geq v_\gamma(t, max(\psi_{\mathrm{car}})), \\ \text{then} \quad & \psi_\gamma = max(\psi_{\mathrm{car}}) \wedge v_\gamma(t, \psi_\gamma) = v_\gamma(t, max(\psi_{\mathrm{car}})) \\ \text{if} \quad & \psi_\gamma \leq -max(\psi_{\mathrm{car}}) \wedge v_\gamma(t, \psi_\gamma) \geq v_\delta(t, -max(\psi_{\mathrm{car}})), \\ \text{then} \quad & \psi_\gamma = -max(\psi_{\mathrm{car}}) \wedge v_\gamma(t, \psi_\gamma) = v_\gamma(t, max(\psi_{\mathrm{car}})) \end{aligned} \tag{11}$$

$$\begin{aligned} \text{if} \quad & -max(\psi_{\mathrm{car}}) \leq \psi_\gamma \leq max(\psi_{\mathrm{car}}) \wedge v_\gamma(t, \psi_\gamma) \geq v_{\gamma\mathrm{empirical}}(\psi_\gamma), \\ \text{then} \quad & v_\gamma(t, \psi_\gamma) = v_{\delta\mathrm{empirical}}(\psi_\gamma) \end{aligned} \tag{12}$$

$$\text{otherwise } \vec{v}_\gamma(t) = \vec{v}_\gamma(t) \tag{13}$$

Equations 10-13 describe the limitation of car movements that can be seen in Figure 5b. Equations 10 and 11 correct $\vec{v}_\gamma(t)$ if the calculated steering angle and corresponding velocity is not executeable by the car driver in reality, whereas Equations 12 and 13 regulates the velocity for the possible steering angle range.

4.4 SFM Extension for Pedestrians

Since the original SFM by Helbing (1991) only considers forces exterted by pedestrians and obstacles onto other pedestrians, forces exerted by vehicles onto pedestrians need to be included as well. The existence of cars in a shared space environment is expressed by a new force term from cars to a pedestrian comparing to the one from neighbourhood pedestrians as it can be seen in Figure 6. This new force explains the most important interaction behaviour of a pedestrian keeping a certain distance to the neighbourhood car since no physical interaction should occur. Therefore, a new socio-repulsive force $\vec{f}_{\alpha\gamma}$ is introduced for the shared space model:

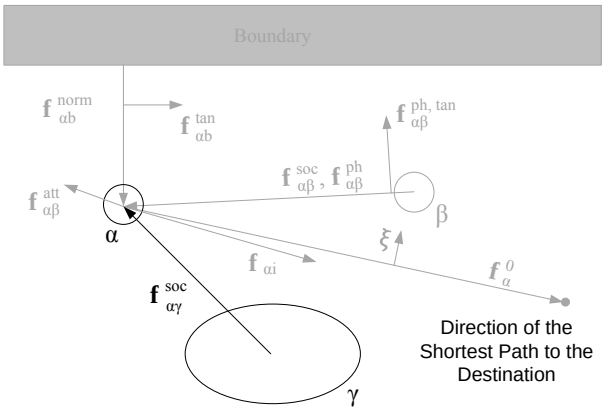

Figure 6: Force Term Exterted from a Car to a Pedestrian

$$\frac{d\vec{v}_\alpha(t)}{dt} = \vec{f}_\alpha^0 + \sum_\beta \vec{f}_{\alpha\beta} + \sum_b \vec{f}_{\alpha b} + \sum_\gamma \vec{f}_{\alpha\gamma} + \vec{\xi} \tag{14}$$

Like the interaction force between pedestrians in the Social Force Model, an exponential function is applied to pedestrian α to represent the influence of distance between the pedestrian and the close-by car γ.

$$\vec{f}_{\alpha\gamma}^{soc} = A_{\alpha\gamma} e^{\frac{r_{\alpha\gamma} - d_{\alpha\gamma}}{B_{\alpha\gamma}}} \vec{n}_{\alpha\gamma} F_{\alpha\gamma} \tag{15}$$

where $r_{\alpha\gamma} = r_\alpha + r_\gamma$; $d_{\alpha\gamma}$ is the distance between the center of pedestrian α and carγ; $\vec{n}_{\alpha\gamma}$ is the normalized vector from car γ to pedestrian α. The form factor $F_{\alpha\gamma}$ is also set similar to 16 to explain the anisotropic behaviour of pedestrian α when facing car γ:

$$F_{\alpha\gamma} = \lambda_\alpha + (1 - \lambda_\alpha)\frac{1 + cos(\varphi_{\alpha\gamma})}{2} \tag{16}$$

Having introduced this microscopic mathematical foundation with the local motion based on social forces, a tactical algorithm is added. This tactical level determines walking or driving paths that human beings are likely to choose under shared space conditions. In fact, the Distance Potential Field is generated separately for pedestrians and drivers to indicate the trajectory of the shortest path to reach the destination (more details will be presented in Anvari et al. (2012).

5 Specification of Parameters and Data Collection

Since the Social Force Model is extended for shared space environments and researchers have only determined the SFM parameters for pedestrians, some new parameters need to be determined by empirical data. Parameters such as the vehicle length $2l$, width $2w$, the steering angle ψ and the effective view angle ϑ can be determined from the technical specification of vehicles. However, the interaction strength A and interaction range B need to be calibrated. The calibration methodology based on real data as well as the extracted data from the video recording of New Road in Brighton is introduced in the following section.

5.1 Methodology of Calibration Process

In order to determine a realistic value for the parameters in the mathematical model for shared environments a certain calibration procedure will be followed (Figure 7). Considering a sim-

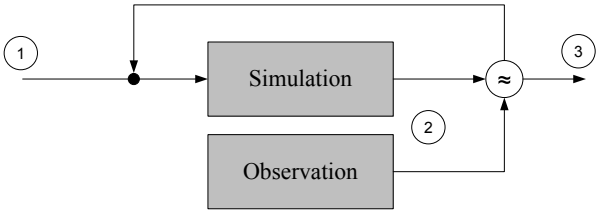

Figure 7: Calibration Procedure for the Parameters A and B

ulation layout similar to the real case study, the observed flow and density is initialised in the simulation program. Parameters such as the desired velocity v_U^0, the length and width of cars $2l$ and $2w$ respectively, the relaxation time τ, the form factor constant λ, the effective view angle ϑ and the steering angle ψ are added. Initial values for the interaction strength A and

1.	Input:	Initial Parameters for A and B.
2.	Output:	Trajectories
		Velocities
		Accelerations and Decelerations
3.	Output:	Calibrated parameters for A and B.

Table 1: Inputs and Outputs for the Calibration for the Parameters A and B

the interaction range B are assumed for the simulation. The output data from the simulation and observation are shown in Table 1. The input and output data are compared and A and B are adjusted. This calibration procedure has to be run unless the compared values fit reality. The simulation can then be evaluated by new observations while the simulation will be up-dated with the correct location of objects. The output values of both will then be compared and analysed.

5.2 Observation of New Road, Brighton

Bidirectional behaviours of pedestrians and drivers were observed in a shared space street in Brighton, United Kingdom (New Road Street, July 2011). The street was video recorded with a digital camera (Panasonic HDC-HS60, 1920x1080 pixels) for one hour and at a height of about 5m (Figure 8a). The picture field covered an area of about 17x160m^2. As it is shown in Figure 8b, a two-meter-wide area on each side of the street was occupied by a few restaurant tables or seats and the main flow of pedestrians and drivers was concentrated

(a) Top View of Area and Camera Position (b) Camera View on Shared Space Area

Figure 8: Layout of New Road in Brighton, United Kingdom

in the middle of the shared space area. 73 pedestrians and 17 vehicles were tracked at a rate of 25$\frac{\text{frames}}{\text{sec}}$ for 5 minutes. In order to extract pedestrian and driver velocity, trajectory, acceleration and deceleration, a recently developed software tool, Trajectory Extractor, is used. The manual measurements with this software involve uncertainties of 0.06m (longitudinal) by 0.02m (lateral) on the near side and 0.55m (longitudinal) by 0.05m (lateral) on the far side (Lee (2007)).

5.3 Parameter Extraction of New Road, Brighton

The observed velocity and acceleration of shared space users in New Road of Brighton is illustrated in Figures 10 and 9. Figure 9a shows that pedestrians accelerate and decelerate

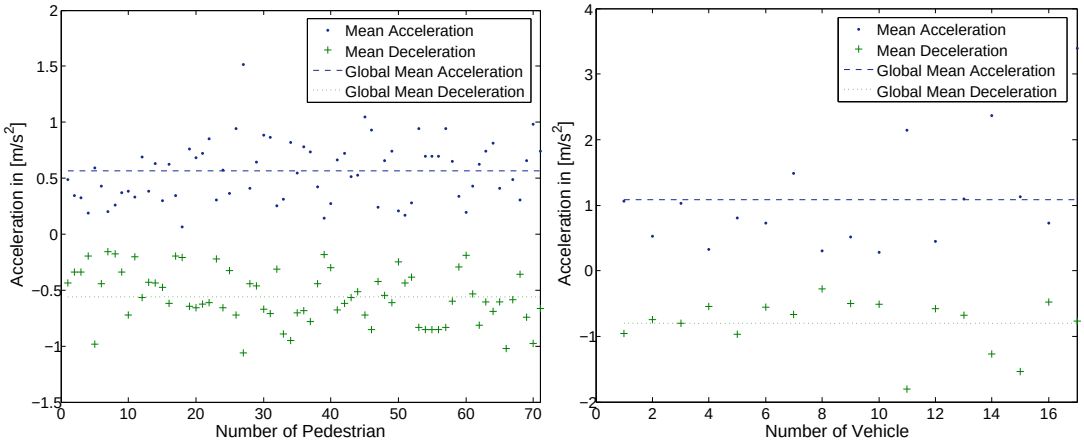

(a) Acceleration Extraction of Pedestrians (b) Acceleration Extraction of Cars

Figure 9: Acceleration Extraction of New Road, Brighton

at almost similar rates of 0.5$\frac{\text{m}}{\text{s}^2}$ which is equivalent to 5% of the g-force. The acceleration and deceleration rate is about 1$\frac{\text{m}}{\text{s}^2}$ for cars in Figure 9b. Therefore, it can be assumed that shared space users are conscious about each other's behaviour as their immediate change of acceleration is low.

According to Figure 10a, the mean of the maximum velocities that pedestrian achieve during their trip is 8.4$\frac{\text{km}}{\text{h}}$ and they walk with the velocity of 4$\frac{\text{km}}{\text{h}}$. The mean of the maximum velocities that cars are driving within this shared street is measured of about 7.2$\frac{\text{km}}{\text{h}}$. As it is shown in Figure 10b, car drivers do not speed up more than 15 $\frac{\text{km}}{\text{h}}$ average which is the aim of sharing space schemes. Further, the observed paths that pedestrian follow within New Road is plotted

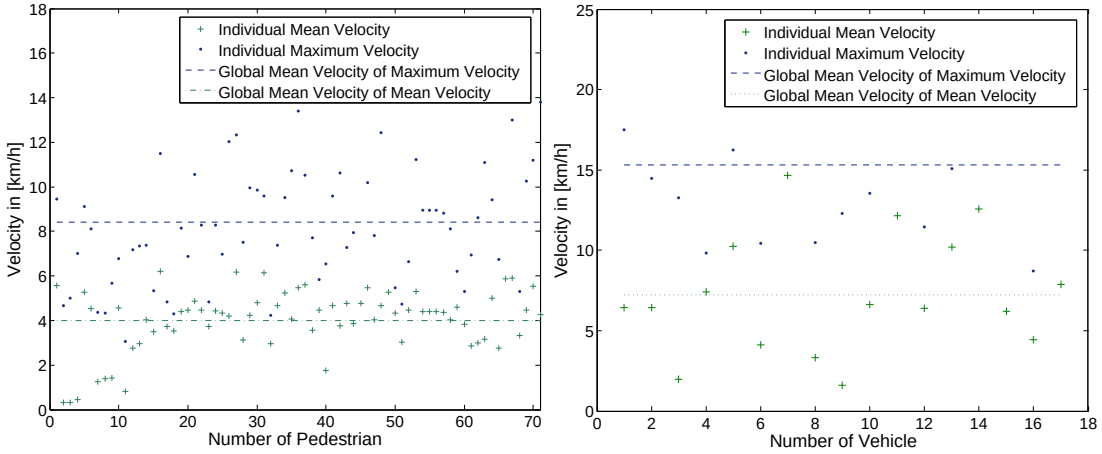

(a) Velocity Extraction of Pedestrians (b) Velocity Extraction of Cars

Figure 10: Velocity Extraction of New Road, Brighton

on the camera view in Figure 11. According to the trajectories, the pedestrian's movements are distributed over the space and the occupancy of the given shared space area is used within its limits.

Figure 11: Trajectories of Pedestrians in New Road, Brighton

6 Conclusions and Future Work

This paper investigates a microscopic mathematical model based on social forces to simulate a shared space system. Since the advanced nature of simulation allows the visualisation of future shared space schemes, the proposed model is developed in C# to validate and improve the basic model and achieve solutions for issues such as optimal traffic capacities or delays. It is shown that the concept of social forces is applicable for modelling the observed movements of shared space users and it facilitates a quantitative prediction of travel patterns. As shared space users traverse the environment, they follow the shortest path which is included in the C# simulation model by defining the information about the static objects within the area in a tactical level. Issues relating to finding the fast path in the environment containing objects which may or may not move will be thought about. The shared space users in Brighton (United Kingdom) are also observed and the data collected is used to initialise the values for the desired velocity, the interaction range B to reach the maximum deceleration and interaction strength A dependently.

Shared space design is used to slow down the traffic flow and create a balance for users waiting times but it performs differently based on the characteristic of the applied area and the used features. A comprehensive qualitative study on the number of interactions, distance of interactions, waiting times, collision time and use of space in different shared space sites is a part of the future work. Also, the calibration of the parameters based on observations from different shared space schemes with different ratio of pedestrians and vehicles will be considered.

Acknowledgements

The author is grateful to Prof. Michael.G.H. Bell and Dr.J. Lee for their valuable help and kind support in providing me resources to carry out the study.

References

Anvari, B., W. Daamen, V. Knoop, S. Hoogendoorn, and M. Bell (2012). Shared space simulation based on social forces and distance potential field. In *6th International Conference on Pedestrian and Evacuation Dynamics*.

Bando, M., K. Hasebe, A. Nakayama, A. Shibata, and Y. Sugiyarna (1995). Dynamical model of traffic congestion and numerical simulation. *Physical Review E 51*, 1035–1042.

Chraibi, M. and A. Seyfried (2010). Generalized centrifugal-force model for pedestrian dynamics. *Physical Review E 82*, 046111.

Franca, R., M. Marietto, W. Santana, and G. Kobayashi (2009). An agent-based simulation model for pedestrian unidirectional movement. In *Second International Conference on the Applications of Digital Information and Web Technologies*.

Ge, H., S. Dai, and L. Dong (2005). An extended car-following model based on intelligent transportation system application. *Physica A 365*, 543–548.

Ge, H., H. Zhu, and S. Dai (2006). Effect of looking backward on traffic flow in a cooperative driving car following model. *The European Physical Journal B 54*, 503507.

Gilman, C. and R. Gilman (2007, June). Shared-use streets: An application of ”shared space” to an american small town. In *3rd Urban Street Symposium*, pp. 1–15.

Hamilton-Baillie, B. (2008). Towards shared space. *Urban Design International 13*(2), 130–138.

Helbing, D. (1991). A mathematical model for the behaviour of pedestrians. *Behavioral Science 36*, 298–310.

Helbing, D., I. Farkas, and T. Vicsek (2000). Simulating dynamical features of escape panic. *Nature 407*, 487–490.

Helbing, D., R. Jiang, and M. Treiber (2005). Analytical investigation of oscillations in intersecting flows of pedestrian and vehicle traffic. *Physical Review E 72*, 0461301–04613010.

Helbing, D. and P. Molnar (1995). Social force model for pedestrian dynamics. *Physical Review E 51*(5), 4282–4286.

Helbing, D. and B. Tilch (1998). Generalized force model of traffic dynamics. *Physical Review E 5*, 133–138.

Ishaque, M. and R. Noland (2007). Trade-offs between vehicular and pedestrian traffic using micro-simulation methods. *Transport Polcy 14 124*, 124138.

Ishii, H. and S. Morishita (2010). A learning algorithm for the simulation of pedestrian flow by cellular automata. *Springer-Verlag Berlin Heidelberg 6350*, 465–473.

Jiang, R. and Q. Wu (2006). Interaction between vehicle and pedestrians in a narrow channel. *Physica A 364*, 239246.

Jiang, R., Q. Wu, and Z. Zhu. (2001). Full velocity difference model for a car-following theory. *Physical Review E 64*, 0171011–0171014.

Lee, T. (2007). *An Agent-Based Model to Simulate Motorcycle Behaviour in Mixed Traffic Flow*. Ph. D. thesis, Imperial College London.

Lewin, K. (1951). *Field Theory in Social Science: Selected Theoretical Papers*. New York: Harper & Row.

Lia, Z. and Y. Liu (2006). Analysis of stability and density waves of traffic flow model in an its environment. *The European Physical Journal B 53*, 367374.

McDonald, M. B. M. (1999). Car-following: A historical review. *Transport Research Part F 2*, 181–196.

Moussad, M., a. S. G. D. Helbing, A. Johansson, M. Combe, and G. Theraulaz (2009). Experimental study of the behavioural mechanisms underlying self-organization in human crowds. *Proceedings of the Royal Society B Biological Sciences 276*, 2755–2762.

Newell, G. (2002). A simplified car-following theory: A lower order model. *Transport Research Part B 36*, 195–205.

Reid, S., N. Kocak, and L. Hunt (2009). Dft shared space project - stage 1: Appraisal of shared space. Technical report, Department of Transport.

Seyfried, A., B. Steffen, W. Klingsch, and M. Boltes (2005). The fundamental diagram of pedestrian movement revisited. *Statistical Mechanics: Theory and Experiment 10*, P10002.

Shearer, D. (2010). Shared spaces in new zealand urban areas. Master's thesis, University of Otago/Te Whare Wananga o Otago.

Xie, D., Z. Gao, and X. Zhao (2009). Stabilization of traffic flow based on multianticipative intelligent driver model. In *International IEEE Conference on Intelligent Transportation Systems*.

Yu, W. J., R. Chen, L. Y. Dong, and S. Q. Dai (2005). Centrifugal force model for pedestrian dynamics. *Physical Review E 72*, 0261121–0261127.

Yu, Y. F. and W. G. Song (2007). Cellular automaton simulation of pedestrian counter flow considering the surrounding environment. *Physical Review E 75*, 0461121–0461128.

Zhang, H. and T. Kim (2005). A car-following theory for multiphase vehicular traffic flow. *Transport Research Part B 39*, 385–399.